Experiment-based determination of the excitation function for the production of ^{44}Ti in proton-irradiated vanadium samples

M. Veicht,[1,2,*] I. Kajan,[1] J.-C. David,[3] S. Chen,[4] E. Strub,[5] I. Mihalcea,[1] and D. Schumann[1]

[1]*Laboratory of Radiochemistry, Paul Scherrer Institut, Forschungsstrasse 111, CH-5232 Villigen, Switzerland*

[2]*École Polytechnique Fédérale de Lausanne (EPFL), Route Cantonale, Lausanne CH-1015, Switzerland*

[3]*IRFU, CEA, Université Paris-Saclay, F-91191, 91190 Gif-sur-Yvette, France*

[4]*Chemistry, Simon Fraser University (SFU), Burnaby, British Columbia, Canada, V5A 1S6*

[5]*Division of Nuclear Chemistry, University of Cologne, Zülpicher Strasse 45, 50674 Cologne, Germany*

(Received 24 February 2021; revised 24 May 2021; accepted 8 June 2021; published 26 July 2021)

In this paper, the excitation function utilizing the nuclear reaction ^{nat}V(p,X) ^{44}Ti was determined. The seven investigated metallic vanadium disks were proton irradiated within an energy range of 111–954 MeV between 1995 to 1996. The experiments' cross sections were validated using two independent measurements by combining γ spectrometry with both a low-energy germanium detector and a high-purity germanium detector. The maximum cross section was observed for energies of 145 ± 1.2 and 150.2 ± 1.2 MeV with values of 803 ± 28 and 805 ± 27 μb, respectively. In this regard, it was demonstrated that our data were in good agreement with the former, however, unpublished results which were investigated over a similar energy range. Thus, combined with these earlier measurements, a consistent data set for the ^{nat}V(p,X) ^{44}Ti excitation function from 111 to 1350 MeV is provided. Model calculations using Liège Intranuclear Cascade (INCL)/ABLA reproduce the shape of the excitation function correctly but overpredict the absolute values by factors of 2 to 3. Some considerations regarding this already earlier observed systematic overestimation of neutron-poor residues are given. The results will trigger new approaches in code development in order to improve the predictions.

DOI: 10.1103/PhysRevC.104.014615

I. INTRODUCTION

The artificial production of the long-lived cosmogenic radioisotope ^{44}Ti was first reported in 1953 [1] whereby scandium oxide was irradiated with 30–45-MeV protons at the Harvard 95-in. synchrocyclotron utilizing the ^{45}Sc(p, $2n$) ^{44}Ti reaction. Since then, studies have focused on accurately determining the nowadays-accepted half-life of 59.1(3) a [2]. Simultaneously, the interest and demand in ^{44}Ti gradually increased over recent years due to the versatility of the radionuclide's field of applications. For instance, lately, the radionuclide is employed in astrophysics [3], e.g., to probe nucleosynthesis environments and, thus, help trace back isotopic abundances at the time of the supernova explosion [4]. Besides, the use for radiopharmaceutical applications is also in the spotlight of research where the interest for ^{44}Ti arises as a possible generator system for the daughter nuclide ^{44g}Sc [$T_{1/2}$ = 3.97(4) h], which serves as a promising nuclide for positron emission tomography [5,6]. The utilization of such a radionuclide generator (^{44}Ti/^{44g}Sc) could conveniently provide ^{44g}Sc. Several strategies were already investigated to design such a generator back in the 1960s–1970s [7, and references therein].

Recent publications report on improved designs, allowing maximal elution of ^{44g}Sc with a minimal breakthrough of parent ^{44}Ti [8,9]. Consequently, its potential off-site availability challenges now the direct ^{44g}Sc production routes using enriched calcium carbonate targets via ^{44}Ca(p, n) ^{44g}Sc [10, and references therein], or alternatively via ^{48}Ti(p,X) ^{44g}Sc [11]. An additional drawback, related to direct production is the inevitable concurrent production of its longer-lived nuclear isomer ^{44m}Sc [$T_{1/2}$ = 58.61(10) h], which obviously complicates patient dosimetry. Thus, it is noteworthy to mention that ^{44m}Sc is not populated in ^{44}Ti decay [6].

Presently, the proton irradiation of high-purity ^{45}Sc metal targets via the ^{45}Sc(p, $2n$) ^{44}Ti reaction is considered as the essential production route for carrier-free ^{44}Ti with reported coherent maxima in the cross sections at around 25 MeV [12–14]. However, its production at intermediate- to high-energy cyclotrons remains expensive and is commercially available only in limited quantities [15].

Even so, the available literature concerning the production of ^{44}Ti remains generally low. In the past, various reactions through the bombardment with accelerated particles have been examined. But, the available overview provided by literature highlights that proton-induced reactions over a wide range of energies and various metal targets were studied. As a result, numerous publications are available covering production cross sections for different residual nuclides (e.g., Refs. [16–19]). However, the formation of ^{44}Ti is not described, and its occurrence seems only rarely investigated. Consequently, carrier-free production of ^{44}Ti is only mentioned concerning iron and nickel targets [18]

*Corresponding author: mario-aaron.veicht@psi.ch

TABLE I. Overview of the vanadium samples analyzed in this paper. The mass was determined based on actual measurements, but mass changes were suspected to partial oxidation of the metal (Fig. 1). Therefore, an averaged disk mass of 132 ± 1.32 mg was used, consistent with the mass from the actual vanadium disks used in the previous work [23].

Sample	Proton energy (MeV)	Proton flux $\times 10^{11}$ (cm^{-2} s^{-1})	Irradiation time (s)	Mass (mg)
VVUH271	111 ± 1.3	1.068 ± 0.021	11400	132.3
VVUL451	129 ± 1.4	1.447 ± 0.024		133.4
VVUL411	134.9 ± 1.3	1.466 ± 0.024		148.3
VVUL333	145 ± 1.2	1.505 ± 0.024	12360	145.9
VVUL291	150.2 ± 1.2	1.523 ± 0.024		140.2
VVUL171	164.5 ± 1.0	1.576 ± 0.024		138.5
VVSN083	954 ± 1.6	0.02430 ± 0.053	60480	151.2

so that the nuclear data on its formation remains almost destitute.

Yet, among all these investigations, the neighboring chemical element vanadium was not considered as a source of ^{44}Ti, although its production was already reported earlier [20]. But, as the authors focused on developing a radiochemical separation method, they did not examine the actual excitation function for the production of ^{44}Ti. Furthermore, even though the interaction of vanadium with protons was investigated in detail [21,22], the production of ^{44}Ti was not considered for the determination of the activation cross sections. But, to find appropriate usage as a target, a detailed knowledge of the excitation function is essential. Natural vanadium consists of two isotopes, namely, for more than 99.75% of vanadium (^{51}V), 0.25% corresponds to the very long-lived ^{50}V ($T_{1/2} = 2.65 \times 10^{17}$ a). As a result, experimental data on $^{\text{nat}}$V can virtually be interpreted in a broad energy range as coming from a monoisotopic ^{51}V target. Thus, the reaction can be referred to as ^{51}V(p, $2p6n$) ^{44}Ti.

Finally, only one publication can be found concerning the measurement of the excitation function for the experimental $^{\text{nat}}$V(p,X) ^{44}Ti, which was published by Zaitseva *et al.* back in 1994 [15]. Here, the authors describe and discuss the possible application of proton irradiated vanadium as a source for a prospective ^{44}Ti/^{44g}Sc generator. Since Ref. [15] investigated the excitation function in the range of proton energies from 54.6 to 100 MeV, our paper allows an extension of the data regarding the experimental production cross section since values in the energy range from 111 to 1350 MeV are presented.

Moreover, as the samples examined here were part of an earlier irradiation campaign, further vanadium specimens that were irradiated during the same campaign are also taken into account [23]. Compared to that data, the advantage of the presented approach is certainly reducing the values' uncertainties utilizing γ-spectrometry measurements with both a low-energy germanium detector (LEGe) and a high-purity germanium detector (HPGe). Both experimentally obtained data sets agree well within the uncertainties. The results are compared with theoretical model calculations.

II. EXPERIMENTAL PROCEDURE

The excitation function for the $^{\text{nat}}$V(p,X) ^{44}Ti reaction was measured using the stacked-foil technique [24]. The irradiation experiments with protons were performed at two facilities in Europe: the Laboratoire National Saturne in Saclay (France) and the Svedberg Laboratory in Uppsala (Sweden). The irradiation took place between October 1995 and March 1996 and covered proton energies ranging from 111 to 954 MeV (Table I). The experiments' initial target preparation was carried out in joint cooperation of the University of Cologne and the Leibnitz University in Hannover. A detailed description of the target preparation can be found elsewhere [24]. The proton fluxes were derived employing the ^{27}Al(p, $3p3n$) ^{22}Na monitor function.

It is noteworthy to mention that the investigated vanadium samples in the present paper were irradiated around 20 yr ago so that short-lived isotopes, occurring from spallation reactions, already decayed and, thus, allowed a precise interference-free detection of ^{44}Ti. Moreover, although a published procedure for the carrier-free separation of tracer ^{44}Ti from proton-irradiated vanadium is available [20], the authors decided in this paper to measure the ^{44}Ti activity without prior chemical separation as by that approach, losses are entirely excluded and, hence, calculating with a 100% yield. Besides, γ-ray attenuation in the dissolved vanadium matrix between 60 to 80 keV was found to be negligible. Furthermore, samples of ^{44}Ti in equilibrium with ^{44g}Sc also allow measuring the 1157-keV line in order to calculate the ^{44}Ti activity.

A. Sample description

The natural metallic vanadium disks (on average: mass ≈ 132 mg, diameter ≈ 1.50 cm, chemical purity of vanadium: 99.8%) (Fig. 1) reference were provided by Goodfellow Cambridge Limited (U.K.). The manufacturer's certificate states typical impurities to be (in parts per 10^6):Cu < 1, Ca < 1, Mg < 1, Mn = 1, Ag = 1, Al = 2, Cr = 15, Fe = 70, and Si = 300.

B. ^{44}Ti reference source

To accurately determine the ^{44}Ti activity of each sample, a calibration source was used that was measured under the same conditions on each of the spectrometers (LEGe and HPGe). At first, the initial specific ^{44}Ti activity of an in-house ^{44}Ti solution (carrier free in 1 M HCl) was measured as a pointlike sample (PLS).

The PLS was prepared by gravimetrically traced droplet deposition (≈20 μl/droplet) using a pycnometer and imme-

TABLE II. Overview of the different reference sources used for the activity determination for different geometries.

Reference	Detector	^{44}Ti activity (Bq/mg)	Added amount (mg)	Total activity (Bq)	Nuclide (energy in keV)
PLS	HPGe	1.140 ± 0.013	86.35 ± 0.01	98.45 ± 1.13	^{44}Sc (1157)
2 mL	LEGe		1021.12 ± 1.02	1161.70 ± 13.42	^{44}Ti (67.9, 78.3)
5 mL	HPGe		1024.26 ± 1.02	1166.47 ± 13.48	^{44}Ti (78.3)

diate evaporation of the solution on a circular polyethylene foil with a diameter of 2.5 cm (specified density = 21.3 ± 1.8 mg × cm^{-2}). The activity concentration of the PLS was determined on the HPGe detector, utilizing the ^{44g}Sc [$T_{1/2}$ = 3.97(4) h] daughter of ^{44}Ti in secular equilibrium with an efficiency of $\varepsilon = 6.88 \times 10^{-4}$ for the 1157-keV line [$I\gamma$ = 99.9(4)%]. The efficiency calibration of the HPGe detector is described elsewhere [25]. Here, ^{44g}Sc was used to derive the ^{44}Ti activity as the emission branching ratio for scandium is precisely known.

Since the PLS was gravimetrically prepared, the stock solution's activity was determined to be 1.140 ± 0.013 Bq/mg (Table II). Consequently, from the calibrated stock solution, two reference sources with volumes of 2- and 5-ml, respectively, were also gravimetrically prepared high-density polyethylene (HD-PE) liquid scintillation counting (LSC) vials. For each sample, 1-ml of the ^{44}Ti stock solution was used, and either 8 M HNO_3 (for the 2-ml reference) or 8 M HCl (for the 5-ml reference) was added to reach the final volume. These solutions were then used for the efficiency calibrations of both LEGe and HPGe detectors to account for the sample-specific geometry.

C. Sample preparation for measurements on LEGe

Initially, each vanadium disk was placed into an HD-PE LSC vial (diameter: 27 mm, height: 58 mm) and dissolved in 2-ml 8 M nitric acid, which was prepared from concentrated nitric acid (Merck KGaA, Germany, Semiconductor Grade MOS PURANAL^{TM}, HNO_3 ⩾ 69%). During the dissolution, the vials were placed in an ice-water mixture to quench the exothermic dissolution reaction. This step was necessary as previous tests with unquenched dissolution experiments showed a solid residue, which was likely due to the formation of vanadium pentoxide (V_2O_5). After the complete disk's dissolution, each sample was subsequently γ spectroscopically measured using the LEGe.

D. Sample preparation for measurements on HPGe

In order to compare the γ-spectrometrical results obtained from the LEGe, a second measurement for each sample on the HPGe system was performed.

However, these measurements were performed several months after the initial measurements. Therefore, each sample was reprocessed to account for changes in the volume, which could have occurred during the sample's storage. Therefore, each HD-PE LSC vial was heated up gently with an open lid to achieve complete dryness. The samples were then treated several times with concentrated hydrochloric acid (Merck KGaA, Germany, ACS reagent, fuming, HCl ⩾ 37%) to dissolve remaining residues on the inner walls of the LSC vial completely.

After another evaporation to dryness, the samples were redissolved using 5-ml of 8 M HCl. This time, HCl was used in order to have a complexing agent, such as chloride, instead of nitrate, as the vanadium metal was already oxidized and, thus, present as V_2O_5. Hence, choosing HCl, V forms various chemically stable and soluble chlorocomplexes [26], ensuring a reliable measurement concerning the geometry as no solids are formed under these elevated HCl concentrations.

E. γ spectroscopy of the Vanadium specimen

γ spectroscopy was conducted using the Canberra LEGe detector and the Canberra BE2825 planar HPGe detector, respectively. The resulting spectra were subsequently analyzed with the Genie2k software (Mirion Technologies, California). The ^{44}Ti reference PLS was measured at a distance of 140(1) mm in air on a 1.2-mm-thick Al support.

As the reference sources from the calibrated solutions were prepared in the same geometry as the measured samples for the activity determination, the efficiency calibration was obtained as counts per second per becquerel of ^{44}Ti activity in the solution of the specified geometry. Such geometry specific calibrations with the same radionuclide diminish both the need for true-coincidence summing corrections and precise knowledge of the photon emission probabilities.

Moreover, a further advantage is given as the knowledge of the efficiency response curve for other energies than nuclide specific ones is not required since it is determined through the count rate at the 67.9- and 78.3-keV γ lines from its decay.

Consequently, this allows comparing the count rate of the calibration solution with the known activity of the same geometry. The final ^{44}Ti activity was projected with a specified reference date (August 30, 2019). The uncertainties are quoted with a coverage factor $k = 1$ (confidence level of about 68%) if not stated otherwise.

F. Theoretical cross-section calculations

Here, the Liège intranuclear cascade model INCL++ [27,28] combined with the de-excitation codes ABLA07 [29] were used to perform theoretical cross-section calculations. This model combination is commonly used to compute the production yields and characteristic particles and nuclei generated in spallation reactions [30]. The progenitors were taken into consideration to calculate the cumulative cross sections as follows:

$$\sigma_{D,\mathrm{cml}} = \sigma_{D,\mathrm{ind}} + \sigma_{M,\mathrm{cml}} \frac{\lambda_M}{\lambda_M - \lambda_D}, \quad (1)$$

TABLE III. Overview of the measured activities of ^{44}Ti from the proton irradiated vanadium disks.

	VVUH271	VVUL451	VVUL411	VVUL333	VVUL291	VVUL171	VVSN083
				$A(^{44}\mathrm{Ti})$ in Becquerels			
LEGe	0.31 ± 0.01	0.55 ± 0.01	0.61 ± 0.01	0.65 ± 0.01	0.67 ± 0.02	0.62 ± 0.01	0.037 ± 0.002
HPGe	0.33 ± 0.01	0.55 ± 0.01	0.64 ± 0.01	0.67 ± 0.01	0.67 ± 0.01	0.69 ± 0.01	0.04 ± 0.01
Unweighted average	0.32 ± 0.02	0.55 ± 0.02	0.62 ± 0.02	0.66 ± 0.02	0.67 ± 0.02	0.65 ± 0.04	0.04 ± 0.01
Uncertainty (%)	5.31	2.84	3.42	2.97	2.74	5.81	15.33

where $\sigma_{D,\mathrm{cml}}$ is the cumulative and $\sigma_{D,\mathrm{ind}}$ is the independent cross section, $\sigma_{M,\mathrm{cml}}$ is the cross section of the parent nuclide, λ_M is the decay constant of the mother, and λ_D is the decay constant of the daughter. Obviously, $\sigma_{M,\mathrm{cml}}$ is calculated, such as $\sigma_{D,\mathrm{cml}}$ making the latter a sum of possibly numerous terms, according to the number of successive progenitors. The details can be found elsewhere [24,30,31].

G. Cross-section determination

Once the activity (A_{sample}) is determined and corrected for the decay time from the irradiation date, the cross-section σ can be calculated, according to a simplified equation,

$$\sigma = \frac{A_{\mathrm{Sample}}\ e^{\lambda t_w}}{N_T\ \Phi_E\ (1 - e^{-\lambda t_{\mathrm{irr}}})}, \tag{2}$$

where λ is the decay constant of the radionuclide, t_w is the time between irradiation (end of beam), and the projected reference date for the γ counting, N_T refers to the number of target atoms, Φ_E represents the proton flux density, and t_{irr} is the irradiation time. In order to compare the past results, the previously determined cross-section values needed to be recalculated. Applying the corrected half-life of ^{44}Ti leads to

$$\sigma^* = \sigma \frac{T^*_{1/2}}{T_{1/2}}, \tag{3}$$

where $T^*_{1/2}$ is the currently accepted half-life [59.1(3) a] and $T_{1/2}$ refers to the half-life used in the cited publications (47.0 a ([15]), and 47.9 a ([23]), respectively), σ represents the former value for the production cross section, and σ^* represents the adjusted value for the comparison (see the Supplemental Material [32])

III. RESULTS AND DISCUSSION

The samples' ^{44}Ti activity as determined by each γ-spectroscopic system, is presented in Table III. For the determination of the cross-section values, the unweighted average of obtained ^{44}Ti activity values were used.

Knowing the integrated proton current and the activity of produced ^{44}Ti, the production cross sections were calculated as displayed in Table IV. Compared with unpublished experimental data [23], investigated over a similar energy range, the presented data show good agreement. Notably, the uncertainties of the obtained cross sections are significantly lower (see the Supplemental Material [32]) in comparison to the data from Protoschill [23] (Fig. 2), whereas only the sample VVSN083 shows a high uncertainty as this is related to the very low ^{44}Ti activity.

For a further comparison concerning the uncertainty values, the error for all the cross sections mentioned in the work of Ref. [15] is stated to be ±20% (Fig. 3) and, thus, considerably higher.

If we compare the experimental data with the predictions of the INCL++ and ABLA 07 codes (Fig. 3), it can be observed that the theoretical data indicate a consistent shift towards much higher cross sections. Generally, the experimental data, thus, suggest that the codes are overestimating the excitation function. Moreover, from the predictions, it can be derived that the maximum is located in the mid-energy range (at 150 MeV), which is consistent with our data.

Accordingly, our data agree with the predicted energy of the maximum cross section with 803 ± 28 μb at an energy in the region of 145 ± 1.2 MeV and with 805 ± 27 μb at 150.2 ± 1.2 MeV. In the work of Ref. [15], the maximum is reached at an energy of 80.8 ± 2 MeV, referring to 830 ± 166 μb. Here, the experimental data differ as by the computational predictions, a global maximum for the cross section is localized at 150 MeV. However, derived from our experimental data, it is obvious that a second maximum is reached at 150 MeV, although the value is not much higher than compared to the maximum value of the lower-energy region.

But, as the values obtained from Ref. [15] are given within a 20% uncertainty, the actual cross-section values in that range might be actually lower so that a global maxium at 150 MeV could be expected. Therefore, a further investigation and, thus, more experimental data in the low-energy region would be required.

TABLE IV. Measured production cross section of ^{44}Ti from the $^{\mathrm{nat}}$V(p,X) ^{44}Ti reaction.

	VVUH271	VVUL451	VVUL411	VVUL333	VVUL291	VVUL171	VVSN083
Energy (MeV)	111 ± 1.3	129 ± 1.4	134.9 ± 1.3	145 ± 1.2	150.2 ± 1.2	164.5 ± 1.0	954 ± 1.6
Cross section (μb)	592 ± 34	697 ± 24	782 ± 31	803 ± 28	805 ± 27	761 ± 46	576 ± 89
Uncertainty (%)	5.77	3.48	3.95	3.55	3.36	6.11	15.52

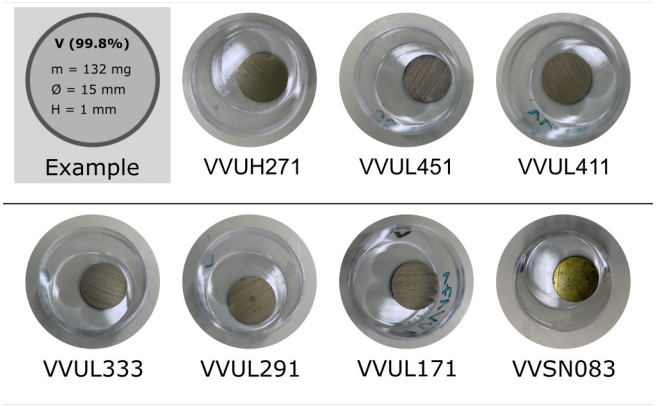

FIG. 1. Overview of the seven metallic vanadium disks before the dissolving process. Notably is the different appearance, which is likely caused by partial oxidation.

Moreover, as the cross sections in the range of greather than 70 MeV are consistently high and even constant in the range from 100 to 150 MeV, also thick targets can be considered for proton irradiations.

Yet, to mention the overestimation of the model, the new data set allows to have a reliable reference for the comparison, based on experimental data. The model's overestimation will require further investigation and, therefore, cannot be corrected in this paper. However, these new data, and others like it, can help to improve the codes. As a preanalysis, we have a first look to the isotopic distribution concerning spallation reaction. It is interesting to estimate the proportion of nuclei with the same proton number (Z) and, in this case, to show the level of difficulty.

For a comparison we use p + Fe for an incident energy of 300–1000 MeV because experimental data exist [33,34] and the production mechanisms are the same as those of ^{nat}V(p,X) ^{44}Ti. As a result, INCL-ABLA compares well with

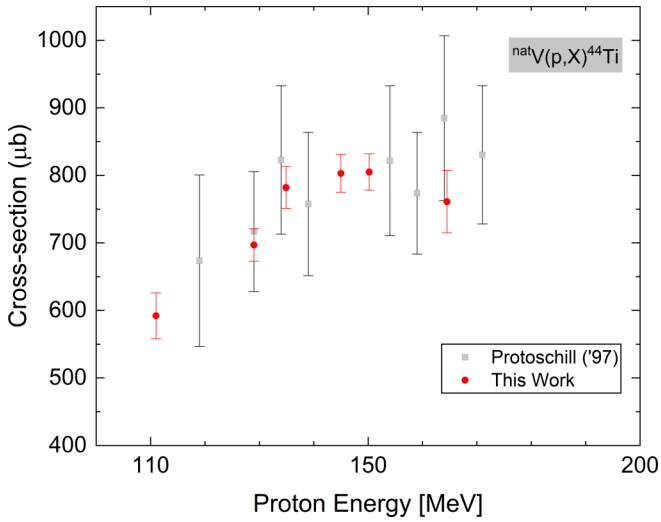

FIG. 2. Experimental excitation function for the ^{44}Ti production from proton-induced reactions as a comparison between the two data sets.

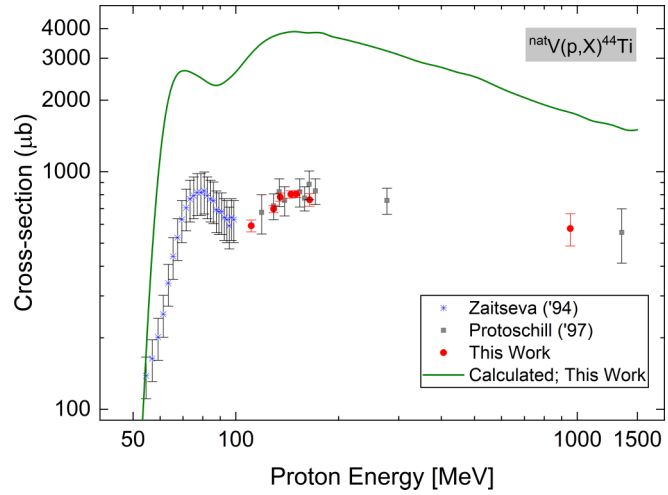

FIG. 3. Further comparison of the excitation function for the ^{44}Ti production with additional data in the low-energy range (taken from Ref. [14]) as well as theoretical calculations.

experimental data (Fig. 4), but there are approximately three orders of magnitude difference between the most produced nucleus ^{54}Mn and the least produced ^{49}Mn. This highlights the difficulty of simulating a nucleus precisely, whose contribution to the global process is so small. Specifically ^{49}Mn is overestimated by a factor of about 3. Consequently, a similar ratio than the one seen for the ^{44}Ti from the p + V reaction is obained.

A second point concerns the ^{52}Fe excitation function of ^{59}Co(p,X) reactions, provided by various sources ([36–42]). Again, the mechanisms to obtain ^{52}Fe from cobalt through proton-induced spallation are analogous to the production of ^{44}Ti from vanadium. Thus, Fig. 5 shows the comparisons between the model and the experiments. Figure 5(a) shows the same overestimation as seen in Fig. 2.

In contrast, the INCL-ABLA results [Fig. 5(b)] are scaled by a factor of 1/3 to focus on the shape of the simulation. In this case, the results of the calculation correspond well to the experiments with a small shift of ∼5 MeV in the low-energy part. This indicates that the overestimation is more or less at the same level independent of the projectile's energy, thus, possibly also not dependent of the excitation energy of the remnant nucleus at the end of the intranuclear cascade.

The following figures also seem to support this view. The first one is related to the previous isotopic distribution. Here, Fig. 6 shows the same mass distributions as seen in Fig. 4 but for several excitation energies at the end of the intranuclear cascade. These new excitation energies have been obtained by multiplying the original excitation energy by factors ranging from 0.5 to 1.5. The good overall results obtained by INCL-ABLA for the residues [43] proved that the excitation energy calculated by INCL has an error probably well below 50%, which ensures that all possibilities are covered here. It seems that the role of the excitation energy is only important for the heaviest isotopes. For our lightest isotope ^{49}Mn, we could see a renewed importance [see Fig. 4(b)]. But, Fig. 7 shows that

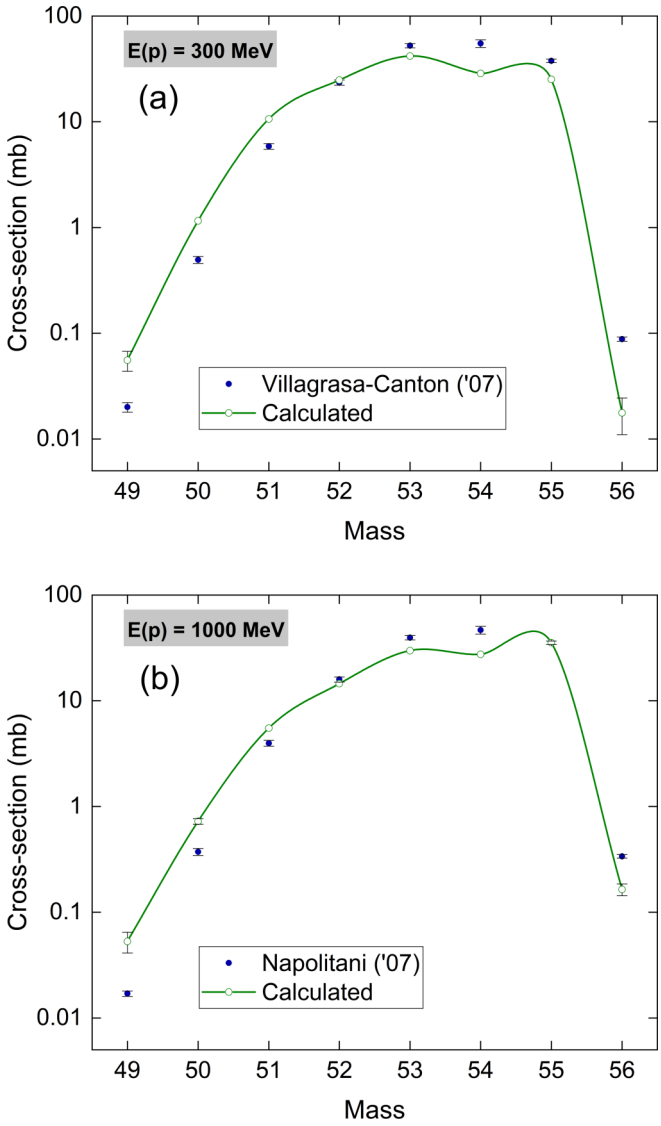

FIG. 4. Mass distributions of the $Z = 25$ isotope from the $p +$ Fe reaction at proton energies (a) $E(p)$ of 300 MeV and (b) $E(p)$ of 1000 MeV. Calculations (green line) come from the INCL-ABLA model combination and experimental data from GSI for 300 MeV [33] and for 1000 MeV [34], respectively.

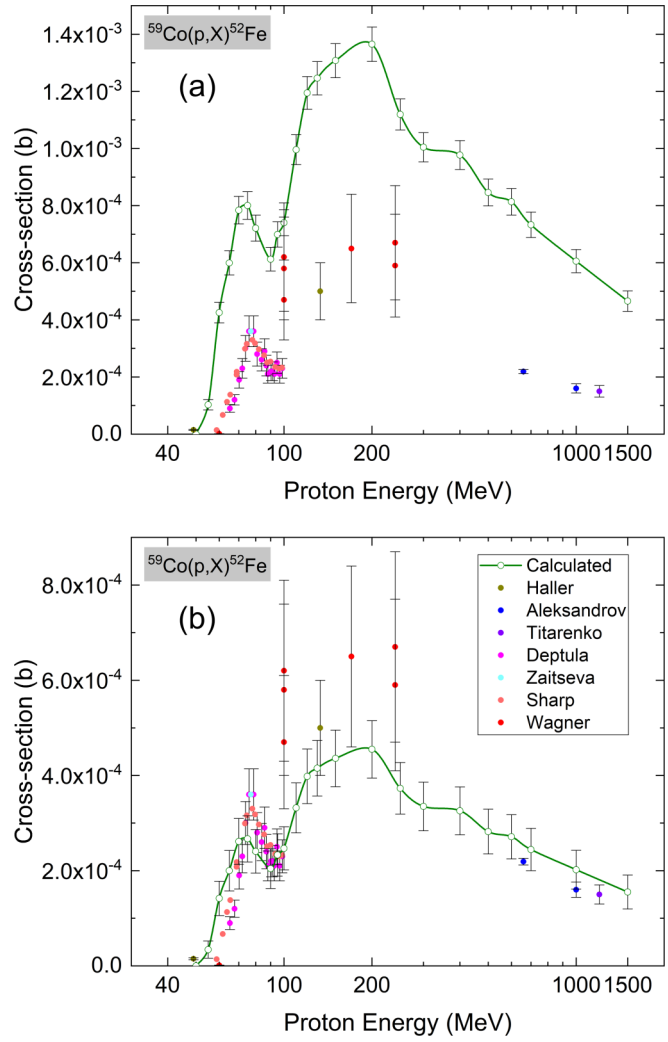

FIG. 5. Compilation of ^{52}Fe excitation function from $p +$ Co reactions. Experimental compiled from [35–41] and theoretical predictions obtained using the INCL-ABLA code combination. Although (a) is the regular comparison in (b) a scale factor of 1/3 is applied to the calculation results.

all excitation energies are compatible with the original value and eventually no clear behaviors emerge.

The second type of figures devoted to the excitation energy concerns its evolution with regard to the projectile energy. This is plotted in Fig. 8 for the reaction $p + {}^{\text{nat}}$V. We can see that the excitation energy varies only slightly with the energy of the projectile by about 30% when the projectile's energy passes from 50 to 1000 MeV and even only about 10% in the specific case of the production of ^{44}Ti. Interestingly, the shape is very similar to the production of ^{44}Ti this being a hint that the excitation energy plays a significant role in the residue production and that INCL simulates it well.

Finally, for the reaction $p + {}^{\text{nat}}$V, many channels or mechanisms are responsible for the production of ^{44}Ti: 19 were identified, but only 12 with a contribution greater than 1%, and 4 greater than 5%. Only these latter ones are summarized in Fig. 9. The very different mechanisms responsible for low- and high-energy productions have in common to emit neutrons during the deexcitation phase. However, ABLA is considered as reliable with regard to neutron emission [43]. We could also suggest that in INCL the ratio of the number of protons emitted to the number of neutrons emitted is too low, thus, leading to an overestimation of the neutron-poor residues. But, the calculated particle spectra seem here again to show that INCL simulates them fairly well [42]. However, this observed overestimation occurs for events with low cross sections, i.e., events that are very sensitive to certain quantities, such as the ones mentioned previously. Particular attention to these quantities will probably be needed to solve the problem.

The measured data discussed here have raised a rather systematic overestimation of neutron-poor residues with INCL-ABLA. They could potentially help to understand the

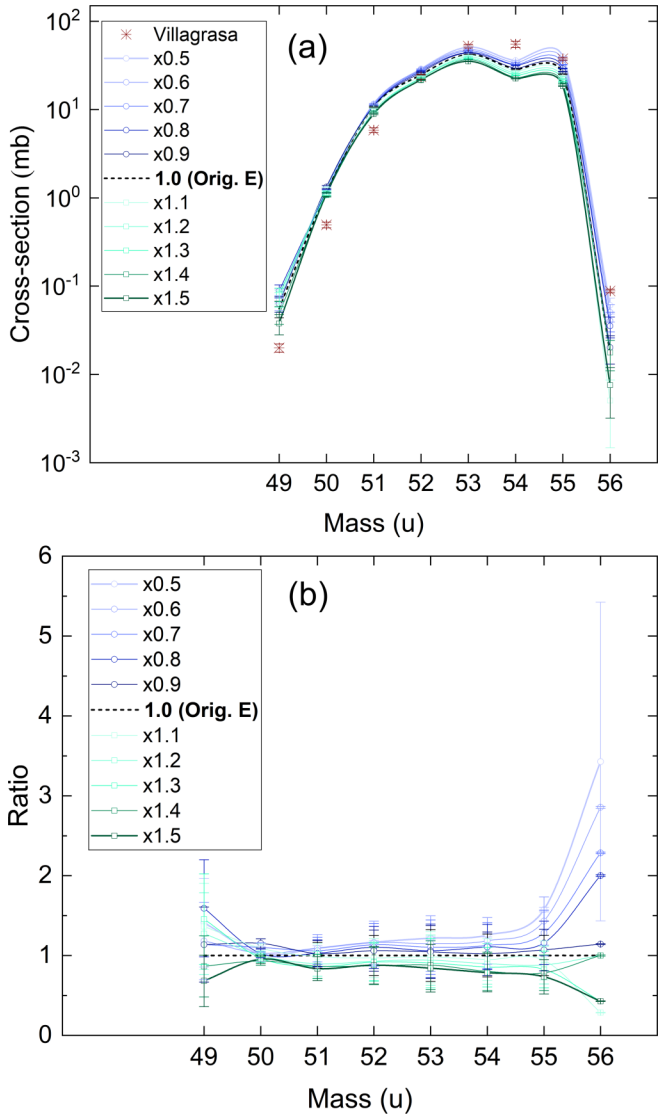

FIG. 6. Mass distributions of the $Z = 25$ isotope from the p + Fe reaction at proton energy $E(p)$ of 300 MeV. Same as Fig. 4, (a) shows where the original excitation energy takes several new values with multiplying factors ranging from 0.5 to 1.5. In (b), the ratios to the original values are plotted. Calculations come from the INCL-ABLA model combination and experimental data from GSI [33].

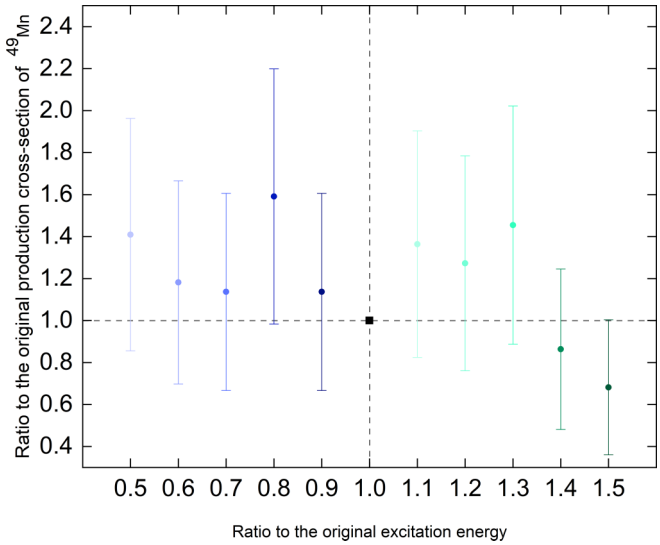

FIG. 7. Evolution of the production cross section of the ^{49}Mn isotope from the p + Fe reaction at proton energy $E(p)$ of 300 MeV including several values of the excitation energy at the end of the intranuclear cascade. Calculations come from the INCL-ABLA model combination.

problem and to improve the calculation results. For instance, a study related to INCL [44] showed that the Bayesian statistics is a powerful tool to estimate the bias of calculated neutron productions. This could be applied to other quantities and especially the residues. In view of this, the data discussed in this paper will play an interesting role.

Finally, we would like to evaluate the potential of a ^{44}Ti/^{44g}Sc generator system obtained by the spallation-based production of the mother nuclide by comparing it with alternative routes to produce the medically interesting ^{44g}Sc.

The production of sufficient amounts of ^{44g}Sc can be achieved either using various direct reactions, including proton, deuteron, and α-particle beams in combination with enriched $^{44}CaCO_3$ and $^{48}TiO_2$ targets, or, alternatively, as the daughter nuclide of the long-lived mother nuclide ^{44}Ti in a ^{44}Ti/^{44g}Sc generator system.

Reported cross sections for the direct production of ^{44g}Sc in the relevant low-energy region (up to 45 MeV) are significantly higher than those for the production of ^{44}Ti. As an example, Ref. [11] calculated several MBq/μAh, regarding the ^{44}Ca(p, n) ^{44g}Sc reaction, whereas [15] reported 0.55 kBq/μAh for the ^{nat}V(p,X) ^{44}Ti. However, this disadvantage is compensated by the possibility for multiusage of the generator system. Although the direct production of ^{44g}Sc requires dedicated beam time for every single batch followed by an ultrafast chemical separation system due to the relatively short half-life of ^{44g}Sc [3.97(4) h], a ^{44}Ti/^{44g}Sc generator can ensure daily delivery within a few minutes over several years. Moreover, the generator avoids the presence of isomeric ^{44m}Sc.

Complementary to the production route via spallation reactions, ^{44}Ti can be produced by proton irradiation of Sc using the ^{45}Sc(p, $2n$) ^{44}Ti reaction. Thick target yields of 5 kBq/μAh were reported [12], calculated for a proton beam with an incident energy of 38 MeV, which is around a factor 10 higher than for the spallation reaction on V. However, the production of a sufficient ^{44}Ti amount using this production path requires several hundred hours of dedicated beam time. As an example: For the production of 370 MBq ^{44}Ti (corresponding to 10 mCi—the smallest unit of the commercially available ^{68}Ge/^{68}Ga generator [45]) using an average cyclotron with 100 μA proton beam current, around 740-h irradiation would be necessary. The follow-up chemical separation of the ^{44}Ti from the matrix material Sc requires extremely high decontamination factors because for the medical application wanted ^{44g}Sc is the same chemical element as the matrix material. Any stable Sc, remaining in the ^{44}Ti fraction, would contaminate the ^{44g}Sc fraction eluted from the generator. This could hinder the labeling to obtain the medically active molecule or, in the

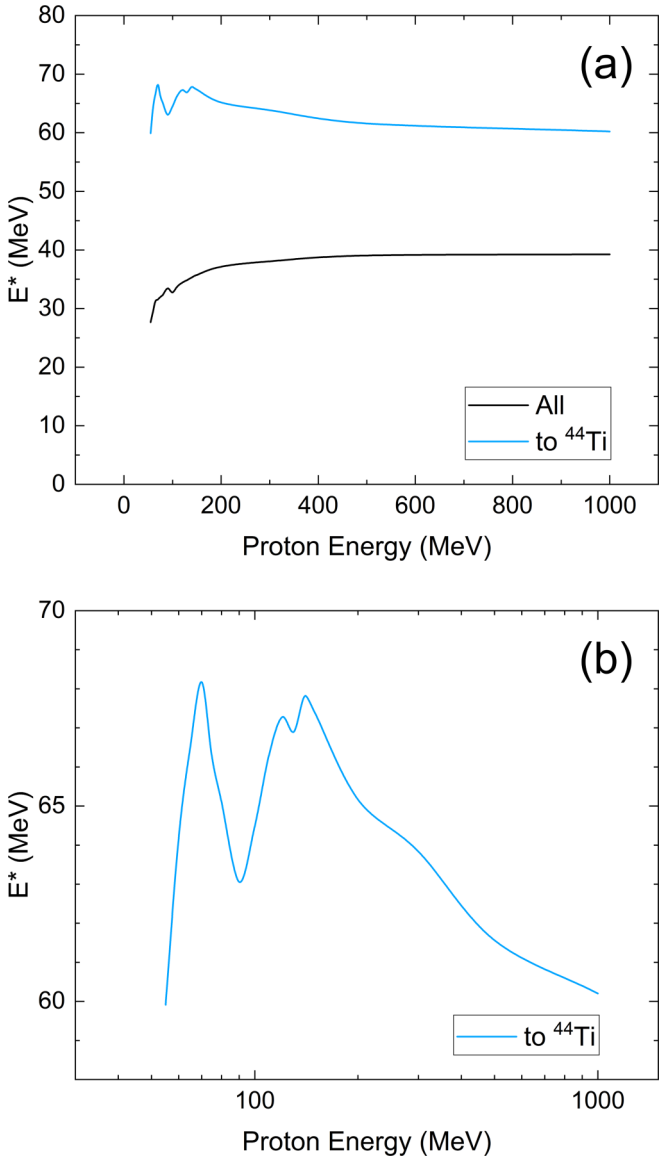

FIG. 8. Excitation energies of the remnant nuclei obtained at the end of the cascade phase for reactions $p + \mathrm{V}$ with proton energies ranging from 50 to 1000 MeV. The black curve shows the mean values for all cases, whereas the blue curve shows only the cases where, at the end of the reaction, a ^{44}Ti nucleus is produced (a). Furthermore, only the latter one is plotted with the X axis in logarithmic representation (b).

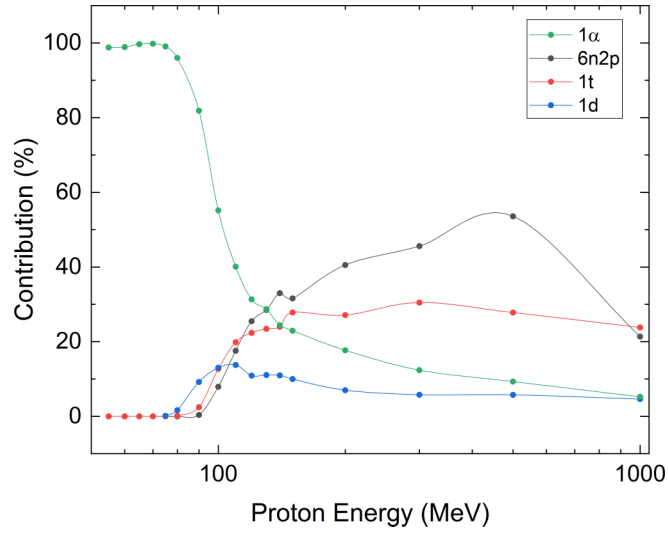

FIG. 9. Contributions to ^{44}Ti production in $p + \mathrm{V}$ reactions with more than 5%. Calculated with the INCL-ABLA combination code. "$6n2p$" means the emission of six neutrons and two protons (in fact, the possible associated emissions of charged pions are included, which obviously modifies the number of neutrons or protons, e.g., seven neutrons + one proton + one π^+ is included). In the same way, "$1d$" means five neutrons, one deuteron, one proton; "$1t$" means four neutrons, one triton, one proton; and "1α" means four neutrons and 1α .

worst case, poison the patient. In view of this, the production route via spallation represents a prospective alternative. As shown in Fig. 3, considerable amounts of ^{44}Ti can be obtained over a relatively wide energy range, this making very thick targets interesting. Given the possibility of dedicated irradiation positions in large-scale spallation facilities, for instance, near the beam dump or at special positions in the spallation target, no extra beam time is required to perform long-term irradiations over several months or even years. The spallation target of the SINQ facility at PSI provides such opportunities. In the frame of the so-called SINQ Target Irradiation Program (e.g., Ref. [46]), around 50g metallic vanadium was irradiated for 2 yr utilizing the high-intensity proton accelerator, resulting in several hundred MBq ^{44}Ti. The radiochemical processing of the V samples is currently in development, leading to a prospective sustainable production of ^{44}Ti/^{44g}Sc. Several high-power spallation sources world wide, such as the Spallation Neutron Source in Oak Ridge (U.S.A.) [47], the Japan Spallation Neutron Source in Tōkai (Japan) [48], TRIUMF in Canada [49] or the still under construction European Spallation Source in Lund (Sweden) [50] are potential sites for such an application.

IV. SUMMARY AND CONCLUSIONS

In this paper, we presented the excitation functions for proton-induced nuclear reactions on seven vanadium disks, concerning the $^{\mathrm{nat}}\mathrm{V}(p,X)$ ^{44}Ti reaction. The presented data support previous experimental results in the energy range of 111–1350 MeV whereas increasing the precision of measured values, employing γ spectroscopy using both a LEGe detector and an HPGe detector. Combined with data from earlier measurements, a consistent data set is presented.

Generally, the measured cross sections over the investigated energy range are overall much lower than predicted by the theoretical calculations. The shape resembles well the trend given by the experimental data, which confirms that the mechanisms responsible for the production seem to be well implemented in the INCL-ABLA codes but are numerically overestimated. The reason for the overall overestimation could lie either in too many remnant nuclei at the end of the intranuclear cascade leading to a ^{44}Ti isotope or in a too easy emission of low-energy neutrons in the evaporation phase of

the deexcitation. More precisely, the correlation between the excitation energy and this excitation function is so strong that one could expect that a few MeVs only could completely change the results. Detailed studies to improve the predictions are planned. The here presented experimental results will help to understand and solve the problems.

The availability of the parent nuclide ^{44}Ti enables the setup of a radionuclide generator that can provide ^{44g}Sc independently and averts the presence of isomeric ^{44m}Sc. Considering the long half-life of ^{44}Ti the generator will provide ^{44g}Sc over a long time span, even if the generator has to be renewed after a certain usage. This circumvents costly beamtimes at accelerator facilities and time-consuming target preparations. A further advantage of a generator is, that ^{44g}Sc can be directly eluted and used, which in addition diminishes activity losses as no further transport or radiochemical separation or purification is required. The exact as possible knowledge of the production cross sections for the production of the mother nuclide is a precondition for the successful commercial implementation of the ^{44}Ti/^{44g}Sc generator system as a reliable medical diagnosis tool in the future.

ACKNOWLEDGMENTS

The authors thank J. Protoschill, whose data we could use for the presented comparison. Also, gratitude to Professor H.-M. Prasser, who was supervising the initial origin of that paper, being a semester work, performed at the Eidgenössische Technische Hochschule Zürich (ETHZ). Moreover, Dr. I.K. thanks Swissnuclear (LRC_20_02) for funding. Dr. I.M. receives funding through the European Union's Horizon 2020 Research and Innovation Program under the Marie Skłodowska-Curie Grant Agreement No. 701647. Furthermore, we acknowledge funding by the Swiss National Science Foundation (SNSF) as part of SINERGIA (Grant No. 177229).

[1] R. A. Sharp and R. M. Diamond, A new titanium nuclide: Ti44, Phys. Rev. **93**, 358 (1954).

[2] J. Chen, B. Singh, and J. A. Cameron, Nucl. data sheets for A = 44, Nuclear Data Sheets **112**, 2357 (2011).

[3] V. Margerin, Transfer reaction measurements and the stellar nucleosynthesis of 26A1 and 44Ti, Doctoral dissertation, Edinburgh University, 2016.

[4] Y. Mochizuki, K. Takahashi, H.-T. Janka, W. Hillebrandt, and R. Diehl, *Titanium-44: Its Effective Decay Rate in Young Supernova Remnants, and its Abundance in Cas A*. arXiv:astro-ph/9904378 (1999).

[5] D. V. Filosofov, N. S. Loktionova, and F. Rösch, A 44Ti/44Sc radionuclide generator for potential application of 44Sc-based PET-radiopharmaceuticals, Radiochim. Acta Int. J. Chem. Aspects Nucl. Sci. Technol. **98.3**, 149 (2010).

[6] F. Roesch, Scandium-44: Benefits of a long-lived PET radionuclide available from the 44Ti/44Sc generator system, Curr. Radiopharm. **5**, 187 (2012).

[7] M. Pruszyński, N. S. Loktionova, D. V. Filosofov, and F. Rösch, Post-Elution processing of 44Ti/44Sc generator-derived 44Sc for clinical application, Appl. Radiat. Isot. **68**, 1636 (2010).

[8] V. Radchenko, C. A. L. Meyer, J. W. Engle, C. M. Naranjo, G. A. Unc, T. Mastren, and M. E. Fassbender, Separation of 44Ti from proton irradiated scandium by using solid-phase extraction chromatography and design of 44Ti/44Sc generator system, J. Chromatogr. A **1477**, 39 (2016).

[9] V. Radchenko, J. W. Engle, D. G. Medvedev, J. M. Maassen, C. M. Naranjo, G. A. Unc, and C. S. Cutler, Proton-induced production and radiochemical isolation of 44Ti from scandium metal targets for 44Ti/44Sc generator development, Nucl. Med. Biol. **50**, 25 (2017).

[10] G. W. Severin, J. W. Engle, H. F. Valdovinos, T. E. Barnhart, and R. Nickles, Cyclotron produced ^{44}gSc from natural calcium, Appl. Radiat. Isot. **70**, 1526 (2012).

[11] M. Sitarz, K. Szkliniarz, J. Jastrzębski, J. Choiński, A. Guertin, F. Haddad, and E. Nigron, Production of Sc medical radioisotopes with proton and deuteron beams, Appl. Radiat. Isot. **142**, 104 (2018).

[12] L. Daraban, R. A. Rebeles, A. Hermanne, F. Tarkanyi, and S. Takacs, Study of the excitation functions for 43K, 43, 44, 44mSc and 44Ti by proton irradiation on 45Sc up to 37 MeV, Nucl. Instrum. Methods Phys. Res., Sect. B **267**, 755 (2009).

[13] V. N. Levkovski, *Cross Sections of Medium Mass Nuclide Activation (*A = 40−100*) by Medium Energy Protons and Alpha Particles (*E = 10−50 MeV*)*, (Inter-Vesi, Moscow, USSR, 1991).

[14] T. McGee, C. L. Rao, G. B. Saha, and L. Yaffe, Nuclear interactions of 45Sc and 68Zn with protons of medium energy, Nucl. Phys. **A150**, 11 (1970).

[15] N. G. Zaitseva, E. Rurarz, M. B. Tchikalov, M. Vobecky, V. A. Khalkin, and L. M. Popinenkova, Production cross sections and yields of long-lived 44Ti from 100 MeV proton bombardment of vanadium, Radiochim. Acta **65**, 157 (1994).

[16] R. Michel, F. Peiffer, and R. Stück, Measurement and hybrid model analysis of integral excitation functions for proton-induced reactions on vanadium, manganese, and cobalt up to 200 MeV, Nucl. Phys. A **441**, 617 (1985).

[17] R. Michel, M. Gloris, H. J. Lange, I. Leya, M. Lüpke, U. Herpers, and P. Dragovitsch, Nuclide production by proton-induced reactions on elements ($6 \leqslant Z \leqslant 29$) in the energy range from 800 to 2600 MeV, Nucl. Instrum. Methods Phys. Res., Sect. B **103**, 183 (1995).

[18] R. Michel, R. Bodemann, H. Busemann, R. Daunke, M. Gloris, H. J. Lange, and S. Neumann, Cross sections for the production of residual nuclides by low-and medium-energy protons from the target elements C, N, O, Mg, Al, Si, Ca, Ti, V, Mn, Fe, Co, Ni, Cu, Sr, Y, Zr, Nb, Ba and Au, Nucl. Instrum. Methods Phys. Res., Sect. B **129**, 153 (1997).

[19] R. Michel and N. Otuka, *Database for proton-induced residual production cross sections up to 2.6 GeV*, International Atomic Energy Agency Report No. INDC (GER)-0052, 2014 (unpublished).

[20] M. Sajjad and R. M. Lambrecht, Separation of tracer titanium-44 from vanadium, Anal. Chem. **58**, 667 (1986).

[21] S. Hontzeas and L. Yaffe, Interaction of vanadium with protons of energies up to 84 MeV, Can. J. Chem. **41**, 2194 (1963).

[22] F. Ditrói, F. Tárkányi, S. Takács, and A. Hermanne, Activation cross-sections of proton-induced reactions on vanadium in the 37–65 MeV energy range, Nucl. Instrum. Methods Phys. Res., Sect. B **381**, 16 (2016).

[23] J. Protoschill, *Untersuchung der Restkernproduktion durch Protoneninduzierte Reaktionen an Schweren Targetelementen* (Diploma Thesis, Leibniz University Hannover, 1997), https://www.irs.uni-hannover.de/fileadmin/irs/Arbeiten/Diplom/diplprot.pdf

[24] M. Gloris, R. Michel, F. Sudbrock, U. Herpers, P. Malmborg, and B. Holmqvist, Proton-induced production of residual radionuclides in lead at intermediate energies, Nucl. Instrum. Methods Phys. Res., Secti. A **463**, 593 (2001).

[25] I. Kajan, S. Heinitz, R. Dressler, P. Reichel, N. Kivel, and D. Schumann, Emission probability of the 66.7 keV γ transition in the decay of Tm 171, Phys. Rev. C **98**, 055802 (2018).

[26] L. D. Kurbatova, T. I. Polupanova, and D. I. Kurbatov, Vanadium(V) complexes in hydrochloric acid solutions, Russ. J. Appl. Chem. **75**, 1216 (2002).

[27] D. Mancusi, A. Boudard, J. Cugnon, J. C. David, P. Kaitaniemi, and S. Leray, Extension of the Liège intranuclear-cascade model to reactions induced by light nuclei, Phys. Rev. C **90**, 054602 (2014).

[28] A. Boudard, J. Cugnon, J. C. David, S. Leray, and D. Mancusi, New potentialities of the Liège intranuclear cascade model for reactions induced by nucleons and light charged particles, Phys. Rev. C **87**, 014606 (2013).

[29] A. Kelic, M. V. Ricciardi, and K.-H. Schmidt, ABLA07-towards a complete description of the decay channels of a nuclear system from spontaneous fission to multifragmentation, arXiv:0906.4193v1.

[30] J. C. David, Spallation reactions: A successful interplay between modeling and applications, Eur. Phys. J. A **51**, 68 (2015).

[31] Y. E. Titarenko, O. V. Shvedov, V. F. Batyaev, E. I. Karpikhin, V. M. Zhivun, A. B. Koldobsky, R. D. Mulambetov, S. V. Kvasova, A. N. Sosnin, S. G. Mashnik, R. E. Prael, A. J. Sierk, T. A. Gabriel, M. Saito, and H. Yasuda, Cross sections for nuclide production in 1 GeV proton-irradiated ^{208}Pb, Phys. Rev. C **65**, 064610 (2002).

[32] See Supplemental Material at http://link.aps.org/supplemental/10.1103/PhysRevC.104.014615 for more detailed error calculations and descriptions.

[33] C. Villagrasa-Canton, A. Boudard, J. E. Ducret, B. Fernandez, S. Leray, C. Volant, and B. Jurado, Spallation residues in the reaction Fe 56 + p at 0.3 A, 0.5 A, 0.75 A, 1.0 A, and 1.5 A GeV, Phys. Rev. C **75**, 044603 (2007).

[34] P. Napolitani, K. H. Schmidt, A. S. Botvina, F. Rejmund, L. Tassan-Got, and C. Villagrasa, High-resolution velocity measurements on fully identified light nuclides produced in Fe 56 + hydrogen and Fe 56 + titanium systems, Phys. Rev. C **70**, 054607 (2004).

[35] I. B. Haller and G. Rudstam, Relative yields of the isomeric pairs ^{69g}Zn – ^{69m}Zn and ^{52g}Mn – ^{52m}Mn in some spallation reactions induced by 20–153 MeV protons, J. Inorg. Nucl. Chem. **19**, 1 (1961).

[36] Y. V. Aleksandrov, A. A. Astapov, S. K. Vasilev, A. Zelinski, R. B. Ivanov, A. Kolachkovski, R. Misiak, M. A. Mikhailova, A. F. Novgorodov, T. I. Popova, and V. P. Prikhodtseva, (1990). Production cross sections of spallation radioactive nuclides in thin targets of Co,Ni,Cu and Zn irradiated by 660 MeV protons, *Conf: 40th All-Union Conference on Nuclear Spectroscopy and Nuclear Structure*, Leningrad, 1990 (Leningrad, Russia, 1990), p. 498.

[37] Y. E. Titarenko, E. I. Karpikhin, A. F. Smolyakov, M. M. Igumnov, O. V. Shvedov, N. V. Stepanov, and T. A. Gabriel, Experimental and calculative research of radioactive nuclei formation-products of target and constructional materials of electronuclear facilities irradiated by protons with energies 1.5 GeV and 130 MeV, in *Proceedings on the Workshop of Exact Measurement in Nuclear Spectroscopy, Sarov, Russia* (1996), p. 184.

[38] C. Deptula, S. H. Kim, S. Mikolajewski, E. Rurarz, L. M. Popinenkova, and N. G. Zaitseva, Excitation functions and yields of some nuclear reactions induced by 100 MeV energy protons in Mn and Co targets: Production of 52 Fe, Nukleonika **35**, 49 (1990).

[39] N. G. Zaitseva, C. Deptula, O. Knotek, K. S. Khan, S. Mikolajewski, P. Mikeć, and L. M. Popinenkova, Cross sections for the 100 MeV proton-induced nuclear reactions and yields of some radionuclides used in nuclear medicine, *Nuclear Data for Science and Technology* (Springer, Berlin/Heidelberg, 1992), pp. 606–608.

[40] R. A. Sharp, R. M. Diamond, and G Wilkinson, Nuclear reactions of cobalt with protons from 0- to 100-MeV energy, Phys. Rev. **101**, 1493 (1956).

[41] G. D. Wagner and E. O. Wiig, Reactions of cobalt with protons at 60, 100, 170, and 240 MeV, Phys. Rev. **96**, 1100 (1954).

[42] J. C. David and I. Leya, Spallation, cosmic rays, meteorites, and planetology, Prog. Part. Nucl. Phys. **109**, 103711 (2019).

[43] S. Leray, J. C. David, M. Khandaker, G. Mank, A. Mengoni, N. Otsuka, and R. Michel, Results from the IAEA benchmark of spallation models, J. Korean Phys. Soc. **59**, 791 (2011).

[44] G. Schnabel, Estimating model bias over the complete nuclide chart with sparse Gaussian processes at the example of INCL/ABLA and double-differential neutron spectra, EPJ Nucl. Sci. Technol. **4**, 33 (2018).

[45] https://radiopharma.com/product/igg100/

[46] W. Wagner, Y. Dai, H. Glasbrenner, M. Grosse, and E. Lehmann, Status of SINQ, the only MW spallation neutron source—highlighting target development and industrial applications, Nucl. Instrum. Methods Phys. Res., Sect. A **562**, 541 (2006).

[47] https://neutrons.ornl.gov/sns

[48] https://j-parc.jp/c/en/index.html

[49] https://www.triumf.ca/

[50] https://europeanspallationsource.se/